The Astrophysical Journal, 615:1063–1072, 2004 November 10
© 2004. The American Astronomical Society. All rights reserved. Printed in U.S.A.

RADIATIVE CHARGE TRANSFER IN COLLISIONS OF O WITH He^+

L. B. Zhao,[1] P. C. Stancil,[1] J. P. Gu,[2] H.-P. Liebermann,[2] Y. Li,[2] P. Funke,[2] R. J. Buenker,[2] B. Zygelman,[3] M. Kimura,[4] and A. Dalgarno[5]

Received 2004 April 27; accepted 2004 July 26

ABSTRACT

Radiative charge transfer has been investigated for collisions of O with He^+ with both a fully quantum mechanical theory and an optical potential method. Cross sections and rate coefficients are presented for the process $O(^3P) + He^+ \rightarrow O^+(^4S^o, ^2P^o, ^2D^o) + He + \hbar\omega$ and are compared to those of direct charge transfer. The relative collision energies considered range from 0.1 meV to ~3 eV with a semiclassical extension to 10 keV and temperatures between 10 and 2.0×10^6 K. The results demonstrate that radiative charge transfer is the dominant process over the energy and temperature region considered. Total emission spectra for the two strongest of the ten possible transitions are given for several collision energies, and the origin of resonance-like structures in the spectra is discussed.

Subject headings: atomic processes — stars: individual (SN 1987A) — supernovae: general

1. INTRODUCTION

Soon after the discovery of supernova SN 1987A, the infrared emission of vibrationally excited CO was detected in its ejecta (e.g., Oliva et al. 1987; Rank et al. 1988). It was recognized through numerous chemical modeling studies that the CO must be formed in the C-O–rich shell of the ejecta with little or no microscopic mixing of lighter elements from outer regions (Lepp et al. 1990; Liu et al. 1992; Liu & Dalgarno 1995; Gearhart et al. 1999). This conclusion is based on the rapid destruction of CO through the dissociative charge-exchange reaction

$$He^+ + CO \rightarrow He + C^+ + O, \quad (1)$$

where He^+ is produced through collisional ionization of helium by energetic electrons created by radioactive decay of ^{56}Co. If helium were present in the C-O zone, then the amount of CO would be substantially reduced, in disagreement with the observations.

However, Lepp et al. (1990) suggested that if charge exchange of He^+ with neutral species (e.g., C, O, Si, S) were rapid, then sufficient He^+ could be removed from the gas to allow for CO formation in elementally mixed ejecta. Because of the lack of experimental or theoretical information on the rate coefficients for these charge-exchange reactions, they postulated various values in order to reproduce the observations. Satisfactory agreement could be obtained if a rate coefficient of 3×10^{-10} cm^3 s^{-1} was adopted for charge transfer of He^+ with O, or alternatively 3×10^{-9} cm^3 s^{-1} for charge transfer with C. More recent unmixed and mixed models by Gearhart et al. (1999) find that the O and C ionization fractions are small ($\sim 10^{-1.5}$ to 10^{-2}) in the C-O zone as a consequence of their relatively large ionization potentials. Therefore, sufficient neutral abundances of O and C are available for CO formation, and also for the possible removal of He^+. If a somewhat larger rate coefficient ($\sim 3.3 \times 10^{-9}$ cm^3 s^{-1}) was adopted for the less abundant species Si and S along with a reduction in the total ionization rate by a factor of 2, the observed CO abundance could also be fitted. Because of their low first ionization potentials, Si and S are found to be nearly completely ionized for the standard ionization rate adopted by Lepp et al. (1990). Furthermore, it is very difficult to estimate rate coefficients for charge exchange involving singly charged ions. These adopted values are highly questionable, requiring either measurements or accurate calculations to make firm conclusions regarding the CO chemistry.

Subsequently, Kimura et al. (1993) calculated the rate coefficient for

$$He^+ + C \rightarrow He + C^+ \quad (2)$$

to be only 5×10^{-14} cm^3 s^{-1} at 2000 K, more than 4 orders of magnitude smaller than that needed in the models of Lepp et al. (1990). The reaction

$$He^+ + O \rightarrow He + O^+ \quad (3)$$

was investigated by Kimura et al. (1994), but was found to have a threshold of ~10,000 K and therefore would proceed at a negligible rate at temperatures relevant to the supernova ejecta. These calculations confirm the modeling studies' arguments that the CO is formed in microscopically unmixed gas. However, this is in contradiction with the failure of the unmixed explosion models to predict the observed emergence of γ-rays and X-rays at early times (Pinto & Woosley 1988).

In this work, we revisit the scheme for removal of He^+ by charge exchange with neutral species by investigating reaction (3). While both processes (2) and (3) are exothermic, Kimura et al. (1993, 1994) considered spin-orbit coupling to be the dominant reaction mechanism. Here, we consider the alternative mechanism of radiative decay, which lacks a threshold.

[1] Department of Physics and Astronomy and Center for Simulational Physics, University of Georgia, Athens, GA 30602-2451; zhao@physast.uga.edu, stancil@physast.uga.edu.

[2] Theoretische Chemie, Bergische Universität Wuppertal, D-42119 Wuppertal, Germany; buenker@uni-wuppertal.de.

[3] Department of Physics, University of Nevada, Las Vegas, NV 89154-4002; bernard@physics.unlv.edu.

[4] Graduate School of Sciences, Kyushu University, Fukuoka 812-8581, Japan; mineoscc@mbox.nc.kyushu-u.ac.jp.

[5] Harvard-Smithsonian Center for Astrophysics, 60 Garden Street, Cambridge, MA 02138; adalgarno@cfa.harvard.edu.

Since CO has been observed in four additional Type II supernovae (Spyromilio & Leibundgut 1996; Gerardy et al. 2000; Spyromilio et al. 2001) and a Type Ic for the first time (Gerardy et al. 2002), having accurate reaction data for the relevant processes becomes more significant. Atomic units are used throughout unless otherwise noted.

2. MOLECULAR ELECTRONIC STRUCTURE CALCULATIONS

The multireference single- and double-excitation configuration-interaction (MRD-CI) method is employed to describe the adiabatic electronic states of the OHe^+ system. The details of this method can be found in Buenker (1982). We choose the same helium atom (Gaussian) basis set as that in our previous study (see Kimura et al. 1994), with a slight modification characterized by $(9s4p1d)/[7s3p1d]$, while the oxygen atom basis set is of the double-ζ plus polarization type $(9s5p1d)/[5s3p1d]$, with added diffuse s, p, and d orbitals with exponents $\beta_s = 0.032$, $\beta_p = 0.028$, and $\beta_d = 0.015$ to yield correct descriptions of the excited states. The potentials of the initial molecular electronic states formed by $O(^3P) + He^+$ and the final states by $O^+(^4S^o, ^2D^o, ^2P^o) + He$ were calculated from the internuclear distance $R = 1.8$ to 9.0 a_0, and the matrix elements of dipole transitions from the initial to final states from $R = 1.5$ to 8.0 a_0.

The 10 adiabatic potential curves are plotted as a function of the internuclear distance R in Figure 1. The four electronic states $2\,^2\Sigma^-$, $3\,^2\Pi$, $2\,^4\Sigma^-$, and $1\,^4\Pi$ are formed by the approach of $O(^3P)$ with He^+; the two states $1\,^2\Sigma^+$ and $2\,^2\Pi$ by $O^+(^2P^o)$ with He; the three states $1\,^2\Delta$, $1\,^2\Pi$, and $1\,^2\Sigma^-$ by $O^+(^2D^o)$ with He; and the state $1\,^4\Sigma^-$ by $O^+(^4S^o)$ with He. The MRD-CI calculated asymptotic energies are presented for the 10 molecular states relative to the $O(^3P) + He^+$ channel and compared with other theoretical and experimental results in Table 1. The computational energies of Simpson et al. (1987) are given relative to the molecular state $2\,^2\Pi$, whose energy is assumed to be the experimental value -5.962 eV. Our results differ with experiment by 5.2%, but are an improvement over those of Simpson et al. (1987).

We extract positions R_m and depths ϵ for the potential wells from the six potential curves for the exit channels. In Table 2, they are compared with those from other ab initio calculations (Simpson et al. 1987; Frenking et al. 1989; Cooper & Wilson 1981; Augustin et al. 1973) and the experimental mobility fits (Viggiano et al. 1993; Viehland & Mason 1977; Lin & Bardsley 1977). Our R_m and ϵ agree with those of the ab initio calculations better than the mobility fits. The table lists the three values, 38.8, 27.3, and 36.3 meV, of the well depth for the $1\,^4\Sigma^-$ state from Simpson et al. (1987). They were obtained with the Hartree-Fock approximation, the MP4SQD method excluding core contributions to electron correlation energies, and the valence bond method, respectively. The last is the most reliable because of the completeness of its theoretical description. However, for the $1\,^2\Pi$ state, Simpson et al. (1987) produced a fit to the experimental mobility by using the valence bond potential well with a depth increased by 20 meV. Thus its well depth is adjusted to be 36.2 meV, which is in good agreement with our value of 33.9 meV. We do not believe that the fit made by Viggiano et al. (1993) to their mobility measurements is optimal. In fact, one can readily infer from their Figure 1, that the fit made by Simpson et al. (1987), rather than that by

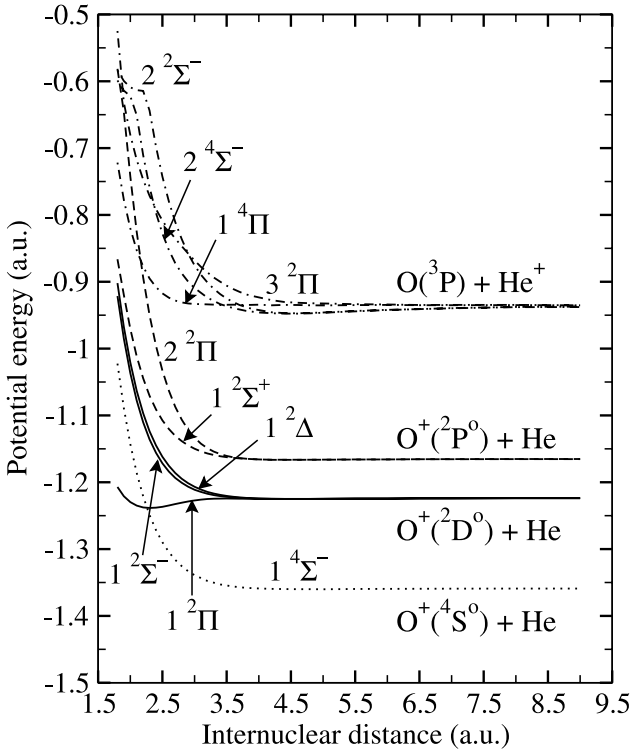

FIG. 1.—Adiabatic potentials of the OHe^+ system. Energies are given relative to -76.0 a.u.

TABLE 1

COMPARISON OF ASYMPTOTIC SEPARATED-ATOM ENERGIES BETWEEN THE PRESENT MRD-CI CALCULATIONS AND OTHERS FOR THE MOLECULAR STATES OF OHe^+

Asymptotic Atomic State	Molecular State	This Work (eV)	Theory[a] (eV)	Experimental[b] (eV)
$O^+(2s^22p^3\,^4S^o) + He$	$1\,^4\Sigma^-$	-11.540	-11.739	-10.979
$O^+(2s^22p^3\,^2D^o) + He$	$1\,^2\Delta$	-7.862		-7.654
	$1\,^2\Pi$	-7.860	-8.215	...
	$1\,^2\Sigma^-$	-7.857		...
$O^+(2s^22p^3\,^2P^o) + He$	$2\,^2\Pi$	-6.269		-5.962
	$1\,^2\Sigma^+$	-6.266		...
$O(2s^22p^4\,^3P) + He^+$	$2\,^4\Sigma^-$	-0.065		0.000
	$2\,^2\Sigma^-$	-0.051		...
	$1\,^4\Pi$	-0.002		...
	$3\,^2\Pi$	0.000		...

[a] Simpson et al. (1987).
[b] NIST Atomic Spectra Database, Web site http://physics.nist.gov/asd.

TABLE 2
POSITIONS AND DEPTHS OF SOME POTENTIAL WELLS FOR THE OHe^+ SYSTEM

	R_m (Å)		ϵ (meV)	
MOLECULAR STATE	This Work	Others	This Work	Others
$1\ ^4\Sigma^-$	2.63	2.42[a]	31.7	38.8
		2.56[a]		27.3
		2.53[a,b]		36.3
		2.00–2.18[c]		51–65
		2.473[d]		35
		2.14[e]		54
		2.13[f]		52
		2.45[g]		31.3
$1\ ^2\Pi$	2.25[i]	2.55[a,b]	38.5	14.5
		2.18[g]		38.8
	1.22[i]	1.25[g]	400	342
		1.32[h]		372
$2\ ^2\Pi$	2.27	2.51[a,b]	33.9	16.2
$1\ ^2\Sigma^-$	2.39		35.9	
$1\ ^2\Sigma^+$	2.41		32.8	
$1\ ^2\Delta$	2.45		32.6	

[a] Simpson et al. (1987).
[b] From the valence bond method.
[c] Viggiano et al. (1993).
[d] Frenking et al. (1989).
[e] Viehland & Mason (1977).
[f] Lin & Bardsley (1977).
[g] Augustin et al. (1973).
[h] Cooper & Wilson (1981).
[i] Our calculations give two potential wells.

Viggiano et al. (1993), better represents their own experimental data. Furthermore, the current MRD-CI calculations give two minima for the $1\ ^2\Pi$ state. The positions and depths of the two wells are in agreement with those of Augustin et al. (1973) as well as the properties of the deeper well with those obtained by Cooper & Wilson (1981).

Beyond $R = 9.0\ a_0$, the potentials are described by the charge-quadrupole and charge-induced dipole interactions,

$$V_L(R) = -\frac{\alpha_\Lambda}{2R^4} + \xi_\Lambda \frac{\langle r^2 \rangle}{R^3} + E_\infty, \tag{4}$$

where α_Λ with $\Lambda = 0, 1, 2, \ldots$ is the dipole polarizability of the neutral atoms, ξ_Λ is an angular parameter, $\langle r^2 \rangle$ is the mean square radius, and E_∞ is the separated-atom energy. The values of α_Λ and ξ_Λ depend on the molecular symmetry. These parameters are taken from Table 2 of Chambaud et al. (1980), and E_∞ is determined using these parameters and the ab initio potentials.

The 10 dipole transition matrix elements $D(R)$ from the four initial molecular states to the six final states are presented as a function of R in Figures 2*a* and 2*b*. The long-range asymptotic behavior of $D(R)$ is fitted to the form d_0/R^n.

3. QUANTAL THEORY OF RADIATIVE CHARGE TRANSFER

A fully quantal approach for radiative charge transfer (RCT) has been formulated by Zygelman & Dalgarno (1988). Here we only outline the theory to evaluate RCT cross sections. The present formulae are not restricted to $\Lambda', \Lambda = 0$ cases for the transition $^{2S+1}\Lambda' \rightarrow {}^{2S+1}\Lambda$, but are applicable to any Λ', Λ that obeys dipole selection rules.

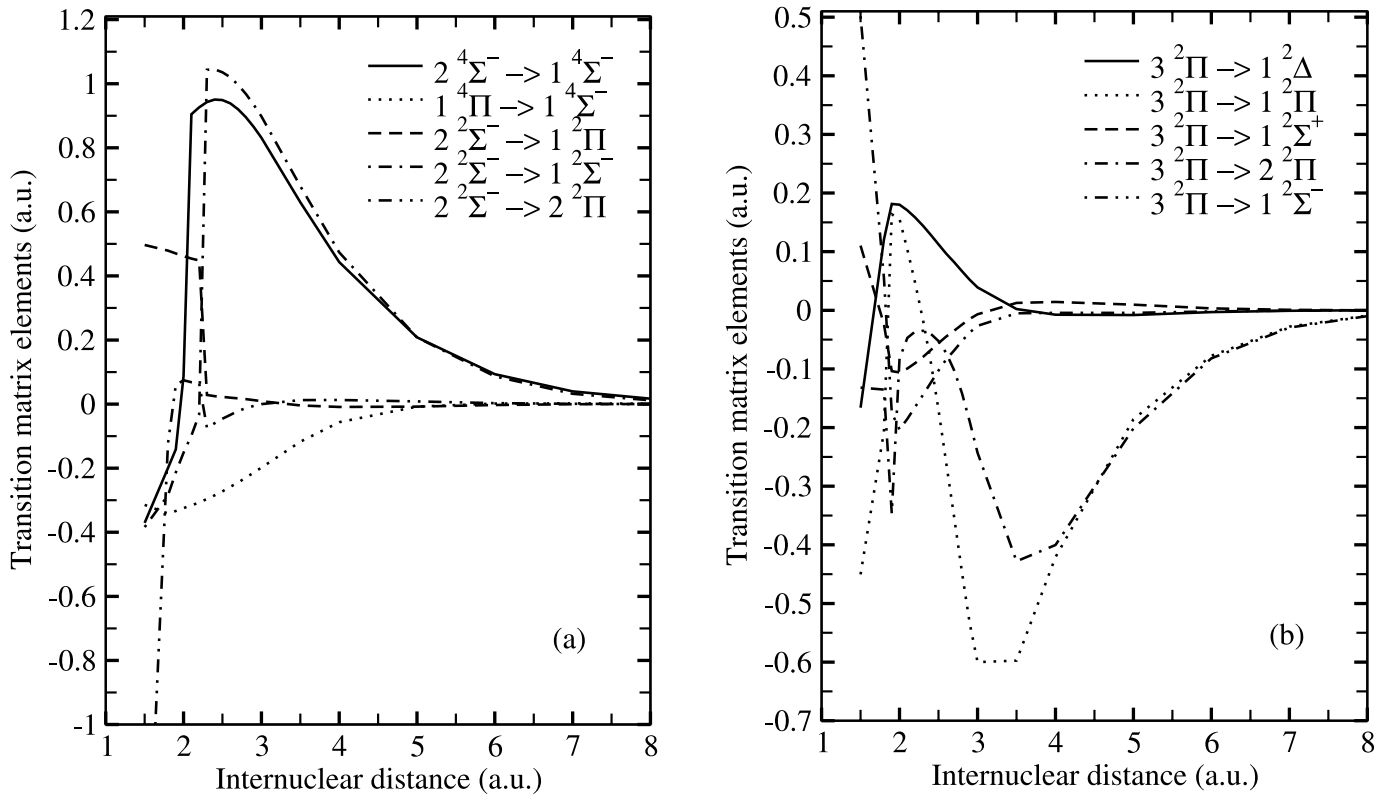

FIG. 2.—Dipole transition moments for OHe^+.

RCT may occur when an atom A and an ion B with electron orbital angular momenta L_A and L_B and spin angular momenta S_A and S_B approach each other. The cross section at relative energy E can be written in the form

$$\sigma(E) = \sum_{\Lambda' S} p_{\Lambda' S} \sigma_{\Lambda' S}(E), \tag{5}$$

where $p_{\Lambda' S} = g_{\Lambda' S}/g_{AB}$ is the probability of approach in any particular molecular state $^{2S+1}\Lambda'$ of spin S and orbital angular momentum projection quantum number Λ', $g_{AB} = (2L_A+1)(2L_B+1)(2S_A+1)(2S_B+1)$, $g_{\Lambda' S} = (2S+1)(2-\delta_{0,\Lambda'})$ (Dalgarno et al. 1990), and

$$\sigma_{\Lambda' S}(E) = \int_0^{\omega_{\max}} \frac{d\sigma}{d\omega}\, d\omega, \tag{6}$$

where $d\sigma/d\omega$ is given by

$$\frac{d\sigma}{d\omega} = \frac{8}{3}\left(\frac{\pi}{k_a}\right)^2 \frac{\omega^3}{c^3} \sum_J \left[S_J^P(\Delta\Lambda)\mathfrak{M}^2_{J,J-1}(k_a,k_b) + S_J^Q(\Delta\Lambda)\mathfrak{M}^2_{J,J}(k_a,k_b) + S_J^R(\Delta\Lambda)\mathfrak{M}^2_{J,J+1}(k_a,k_b)\right], \tag{7}$$

where

$$\mathfrak{M}_{J,J'}(k_a,k_b) = \int_0^\infty dR f_J^a(k_a R) D(R) f_{J'}^b(k_b R). \tag{8}$$

The wavenumbers for center-of-mass motion of the initial and final ion-atom channels are k_a and k_b, respectively, ω is the angular frequency of the emitted photon, c is the speed of light, J is the total angular momentum of the molecular system, $S_J^X(\Delta\Lambda)$ where X is P, Q, or R represents the Hönl-London factor (see the Appendix), $D(R)$ is the dipole transition moment from an initial state to a final state, and f_J^x, where x is a or b, is the regular solution of the radial Schrödinger equation

$$\left\{ \frac{d^2}{dR^2} - \frac{J(J+1)-\Lambda^2}{R^2} - 2\mu[V_x(R) - V_x(\infty)] + k_x^2 \right\} f_J^x(k_x R) = 0, \tag{9}$$

$$k_a = \sqrt{2\mu[E - V_a(\infty)]}, \tag{10}$$

$$k_b = \sqrt{2\mu[E - V_b(\infty) - \hbar\omega]}, \tag{11}$$

where μ is the reduced mass of the molecular system, V_a and V_b denote the adiabatic potential energies of the entrance and exit channels, respectively, and f_J^x is normalized asymptotically according to (e.g., Stancil & Zygelman 1996)

$$f_J^x(k_x R) \approx \sqrt{\frac{2\mu}{\pi k_x}} \sin\left(k_x R - \frac{J\pi}{2} + \delta_J^x\right), \tag{12}$$

where δ_J^x denotes the channel phase shifts. Here we have neglected the spin angular momentum and made the approximation that for large J, the factor in equation (9)

$$J(J+1) - \Lambda^2 \approx L(L+1), \tag{13}$$

where L is the total orbital angular momentum given by

$$L \approx J - 2\Lambda^2/(1+2J), \tag{14}$$

which is equal to J for large J. We stress that equation (12) is strictly correct for $\Lambda = 0$ states, but it is an approximation for $\Lambda = 1, 2, \ldots$ states. The radial Schrödinger equation of nuclear motion, equation (9), can be numerically solved for both the entrance and exit channels, and total RCT cross sections can be obtained by integrating over the total spectrum in the fully quantal approach.

An approximation, the so-called optical potential method, can be adopted to obtain the total cross sections for collision-induced radiative decay including both RCT and radiative association. The central idea of the approximation is that the nonlocal potential, which stems from the interaction of the electrons with the radiation field, is semiclassically approximated by a local potential in the eigenvalue equations. The total cross section for radiative decay from a molecular state $^{2S+1}\Lambda'$ at relative collision energy E can be written in this approximation as (Zygelman & Dalgarno 1988)

$$\sigma_{\Lambda' S}(E) = \frac{\pi}{k_a^2} \sum_J^\infty (2J+1)[1 - \exp(-4\eta_J)], \tag{15}$$

where η_J is the imaginary part of the phase shift of the Jth partial wave of the radial Schrödinger equation, which is given in the distorted-wave approximation by

$$\eta_J = \frac{\pi}{2} \int_0^\infty dR \left| f_J^a(k_a R) \right|^2 A(R), \tag{16}$$

where

$$A(R) = \frac{4}{3} D^2(R) \frac{|V_b(R) - V_a(R)|^3}{c^3}. \tag{17}$$

To obtain the total cross section for collision-induced radiative decay, the solution of the radial Schrödinger equation is only required for the entrance channel.

4. RESULTS AND DISCUSSION

The molecular data described in § 2 were employed to calculate the total cross sections for collision-induced radiative decay and are shown in Figures 3*a* and 3*b*. The cross sections for all 10 transitions were obtained with the optical potential method. The region of the relative collision energy considered is from 0.1 meV to ~3 eV. The open circles represent cross sections for RCT obtained with the fully quantal approach. The cross sections for the different transitions vary in magnitude over a wide range. A drop in the cross section occurs at ~1.2 meV for all transitions that originate in either the $1\,^4\Pi$ or $3\,^2\Pi$ states. The drop is due to a potential barrier in the initial state as a consequence of the quadrupole term in the long-range expansion given in equation (4). The barrier has a height of 1.17 meV at $R = 11.75$ a.u. in both states. The cross section drops at higher energies are likely related to artifacts in the $1\,^4\Pi$ or $3\,^2\Pi$ potentials.

Figure 3 illustrates that the two dominant transitions are due to $2\,^4\Sigma^- \rightarrow 1\,^4\Sigma^-$ and $2\,^2\Sigma^- \rightarrow 1\,^2\Sigma^-$ for the RCT process. For four of the transitions in Figure 3*a*, except for the $1\,^4\Pi \rightarrow 1\,^4\Sigma^-$, the background cross section, excluding resonances, decreases monotonically by more than 2 orders of magnitude

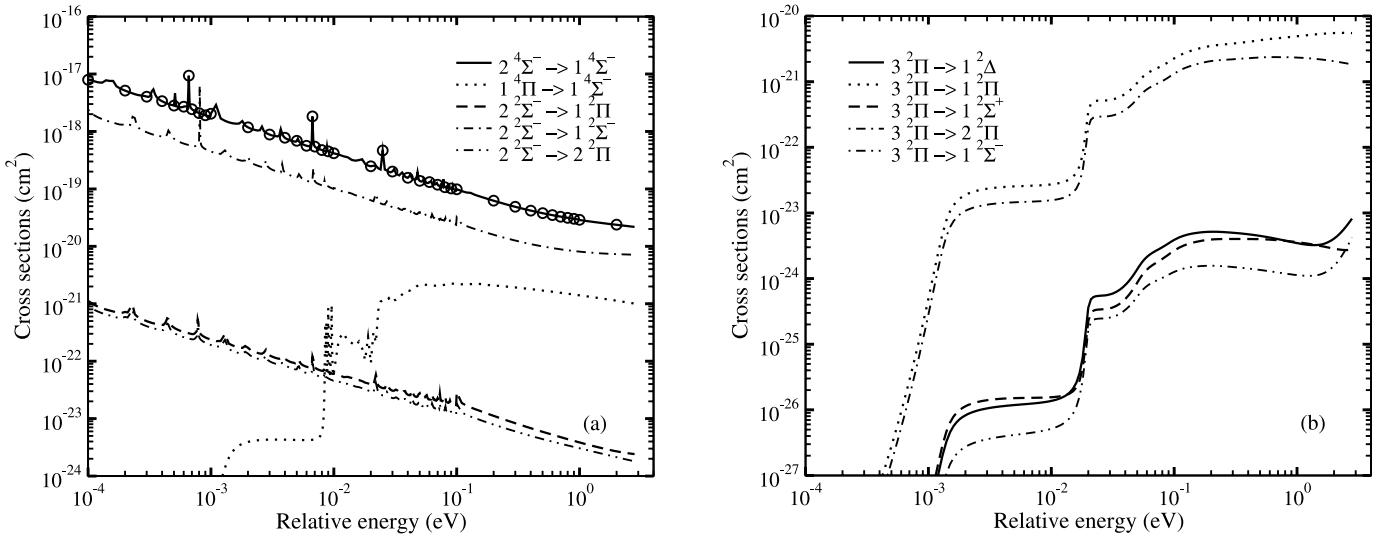

FIG. 3.—Cross sections for radiative decay as a function of collision energy. All the curves are calculated with the optical potential method (eq. [15]), while the calculations using the fully quantum mechanical method (eq. [7]) are given as open circles. The cross sections do not include the approach probability factor $p_{\Lambda S}$.

as the relative collision energy increases from 0.1 meV to $\sim$3 eV. Differing from the other six transitions, the four curves do not display sudden drops. This is because the initial molecular states, $2\,^4\Sigma^-$ and $2\,^2\Sigma^-$, are purely attractive at long range, rather than possessing potential barriers. In Figure 3*a*, one may find the presence of the resonance structures in the energy region between 0.1 and 100 meV. These resonances are attributed to the presence of quasi-bound levels in the entrance channel. The resonances for the transitions, $2\,^2\Sigma^- \rightarrow 1\,^2\Pi$, $2\,^2\Sigma^- \rightarrow 1\,^2\Sigma^-$, and $2\,^2\Sigma^- \rightarrow 2\,^2\Pi$, all with the same initial state $2\,^2\Sigma^-$, appear in the exact same positions. The resonances may give rise to an enhancement in the rate coefficients. In the higher energy region, the cross sections become smooth, lacking any resonance structure. We note that the molecular states $2\,^4\Sigma^-$ and $2\,^2\Sigma^-$ for the entrance channels of the two dominant transitions possess potential wells less than 0.3 eV, and therefore are weakly bound. One does not expect quasi-bound levels or orbiting to exist for energies higher than this value (Mott & Massey 1965; Zygelman et al. 1989).

The cross sections for the collision-induced radiative decay, which have been multiplied by the probability factor $p_{\Lambda' S}$, are compared with those for direct charge transfer from Kimura et al. (1994) in Figure 4. Our cross sections for radiative decay to $O^+(^4S^o) + He$, $O^+(^2P^o) + He$, $O^+(^3D^o) + He$, and a summation of these three channels owing to collisions of $O(^3P)$ with He^+ are plotted as a function of relative energy. As the cross sections for direct capture to the ground state $^4S^o$ and the metastable state $^2D^o$ of O^+ are negligible, only the cross sections for capture to the metastable $O^+(^2P^o)$ are displayed for comparison.

In order to extend to higher energy, we also carried out semiclassical calculations of the cross sections for radiative decay. The present calculation starts from 0.1 eV and extends to 10^4 eV for all 10 transitions. The semiclassical cross section is determined by the relation (Zygelman & Dalgarno 1988)

$$\sigma(E) = 2\pi\sqrt{\frac{2\mu}{E}} \int p\,dp \int_{R_a^{\rm ctp}}^{\infty} dR\, \frac{A(R)}{\sqrt{1 - V_a(R)/E - p^2/R^2}}, \tag{18}$$

where p is the impact parameter and $R_a^{\rm ctp}$ is the classical turning point in the incoming channel. The partial cross sections for radiative decay to the three final channels and the total cross section are presented in Figure 4. It is noted that even at $E = 0.1$ eV, the semiclassical approximation produces results in excellent agreement with those from the quantal method. For large energies ($E \gg V_a$), the double integral is nearly energy independent and therefore $\sigma(E)$ varies as $1/\sqrt{E}$. Our numerical results for all the transitions display such behavior for $E \gtrsim 30$ eV, as seen in the figure. The cross section for direct electron capture has a maximum value of 1.5×10^{-21} cm^2 at 8 eV, but decreases quickly with decreasing relative energy giving 1.01×10^{-24} cm^2 at 2.67 eV. It is obvious that at energies below 2.7 eV, the contribution from direct charge transfer to form $O^+(^4S^o, ^2P^o, ^2D^o)$ in the collision of $O(^3P)$ with He^+ is negligible. Even at $E = 8$ eV, where the direct

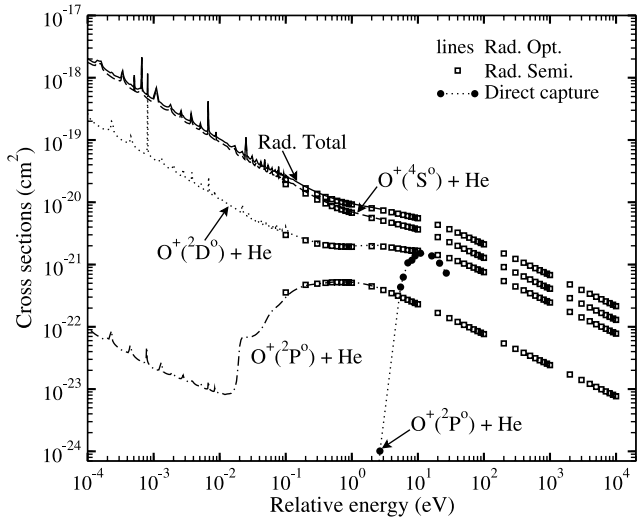

FIG. 4.—Comparison of the cross sections for radiative decay with those for direct electron capture for collisions of $O(^3P)$ with He^+. Radiative decay obtained with the optical potential method (*curves*), radiative decay obtained with semiclassical approximation (*open squares*), and direct charge transfer from Kimura et al. (1994) (*filled circles*).

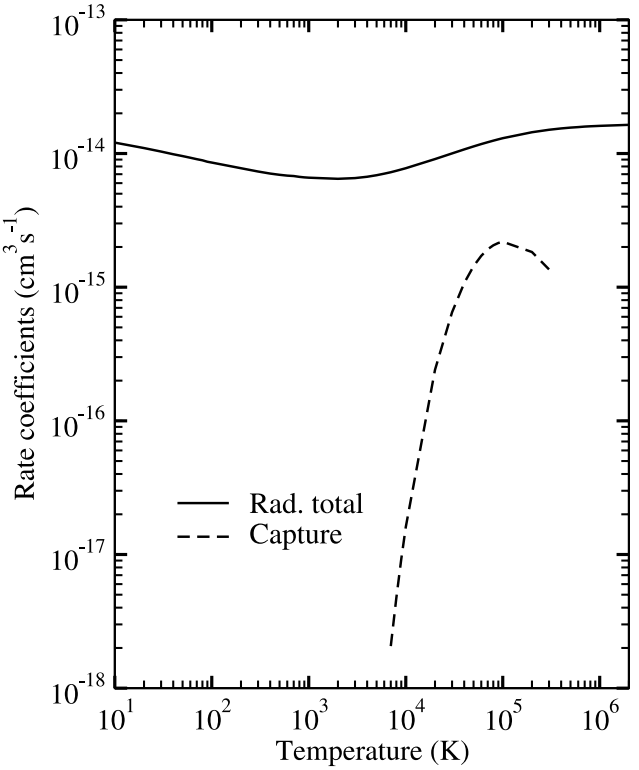

FIG. 5.—Comparison of the total rate coefficients for radiative decay (*solid line*) with those for direct charge transfer from Kimura et al. (1994) (*dashed line*), obtained by averaging the cross sections in Fig. 4 with a Maxwellian velocity distribution for collisions of O(^3P) with He^+.

capture cross section is at a maximum, the contribution to charge transfer from radiative decay is more significant than that from direct electron capture.

Rate coefficients were obtained by averaging the cross sections in Figure 4 over a Maxwellian velocity distribution and are plotted as a function of temperature T in Figure 5. The solid and dashed lines denote radiative decay and direct charge transfer, respectively. Below 10^4 K the rate coefficients for direct charge transfer are negligible, but it increases sharply for higher temperatures and reaches a maximum value of 2.2×10^{-15} cm^3 s^{-1} at 1.0×10^5 K. Even so, the importance of direct charge transfer is not comparable to that of radiative decay for the studied temperature range. Above $\sim 5 \times 10^5$ K, the rate coefficient for radiative decay approaches a constant with increasing T. This is because the cross section behaves as $1/\sqrt{E}$ at large energies. We also tabulate the rate coefficients for collision-induced radiative decay between 10 and 1×10^6 K in Table 3. For convenience, the rate coefficients are fitted to the form

$$\alpha(T) = \sum_i a_i \left(\frac{T}{10,000}\right)^{b_i} \exp\left(-\frac{T}{c_i}\right). \qquad (19)$$

The fitting parameters are given at the end of Table 3. Units for a_i and c_i are cm^3 s^{-1} and K, respectively. The fit does not deviate from the computed rate coefficients by more than 6%.

The total emission spectra $d\sigma/d\omega$ for the RCT process $O(^3P) + He^+ \rightarrow O^+(^4S^o, ^2P^o, ^2D^o) + He + \hbar\omega$ were also evaluated. The contributions from the individual incoming partial waves J are summed as in equation (7) until a convergence of $d\sigma/d\omega$ is achieved. In Figure 6, we present the total emission

TABLE 3

TOTAL RATE COEFFICIENTS FOR RADIATIVE CHARGE TRANSFER
$O + He^+ \rightarrow O^+ + He + \hbar\omega$

T (K)	$\alpha(T)$[a] (cm^3 s^{-1})	T (K)	$\alpha(T)$ (cm^3 s^{-1})
10	1.21(−14)	6000	7.06(−15)
20	1.10(−14)	7000	7.24(−15)
30	1.03(−14)	8000	7.43(−15)
40	9.88(−15)	9000	7.60(−15)
50	9.57(−15)	10,000	7.76(−15)
60	9.29(−15)	20,000	9.08(−15)
70	9.07(−15)	30,000	1.00(−14)
80	8.90(−15)	40,000	1.07(−14)
90	8.68(−15)	50,000	1.13(−14)
100	8.56(−15)	60,000	1.18(−14)
200	7.77(−15)	70,000	1.22(−14)
300	7.34(−15)	80,000	1.25(−14)
400	7.08(−15)	90,000	1.28(−14)
500	6.94(−15)	100,000	1.30(−14)
600	6.83(−15)	200,000	1.44(−14)
700	6.79(−15)	300,000	1.50(−14)
800	6.69(−15)	400,000	1.54(−14)
900	6.63(−15)	500,000	1.56(−14)
1000	6.60(−15)	600,000	1.58(−14)
2000	6.47(−15)	700,000	1.59(−14)
3000	6.54(−15)	800,000	1.60(−14)
4000	6.70(−15)	900,000	1.61(−14)
5000	6.88(−15)	1,000,000	1.61(−14)
a_1	4.991(−15)	a_2	2.780(−15)
b_1	0.3794	b_2	−0.2163
c_1	1.121(+06)	c_2	−8.158(+05)

NOTES.—Fitting parameters a_i, b_i, and c_i in equation (19) are given at the end of the table. Units for a_i and c_i are cm^3 s^{-1} and K, respectively.

[a] $A(-B) = A \times 10^{-B}$.

spectra for the two strongest transitions for collision energies of 0.1, 1, 10, and 100 meV. The spectra for the transition $2\,^4\Sigma^- \rightarrow 1\,^4\Sigma^-$ are displayed in Figures 6*a* and 6*b*, while those for $2\,^2\Sigma^- \rightarrow 1\,^2\Sigma^-$ are given in Figures 6*c* and 6*d*. Each emission spectrum starts from a minimum value of the wavelength $\lambda_{\min}$ and theoretically extends to infinity. Actually, it is quickly attenuated, as observed in these figures, since $d\sigma/d\omega$ depends on λ^{-3}. The wavelength λ is related to the outgoing wavenumber k_b by energy conservation (Zygelman et al. 1989),

$$\frac{2\pi c}{\lambda} = \frac{k_a^2}{2\mu} + V_a(\infty) - \frac{k_b^2}{2\mu} - V_b(\infty). \qquad (20)$$

From equation (20), $\lambda_{\min}$ for a given k_a corresponds to $k_b = 0$, and $\lambda = \infty$ corresponds to $k_b = \{k_a^2 + 2\mu[V_a(\infty) - V_b(\infty)]\}^{1/2}$.

The emission spectra show some resonance-like structures. For example, in Figures 6*a* and 6*b*, $d\sigma/d\omega$ has a main peak at $\lambda = 1097.7$ Å when the relative collision energy is 0.1 meV. The dominant peak shifts to longer λ, and its height is reduced with increasing collision energy from 0.1 meV to 100 meV. The structures of the emission spectra are determined by phase differences between incoming and outgoing waves at small and intermediate internuclear distances ($R < 10$ a.u.), where dipole transition moments are not negligible. If the phase difference equals approximately $n\pi$ (here n is an integer), the overlap integral $\mathfrak{M}_{J,J'}$ is enhanced, and it is reduced if the phase difference equals $(n + 1/2)\pi$. For a given E in the entrance channel, the phase difference varies with the change of the outgoing wavenumber k_b, which is related to the frequency of

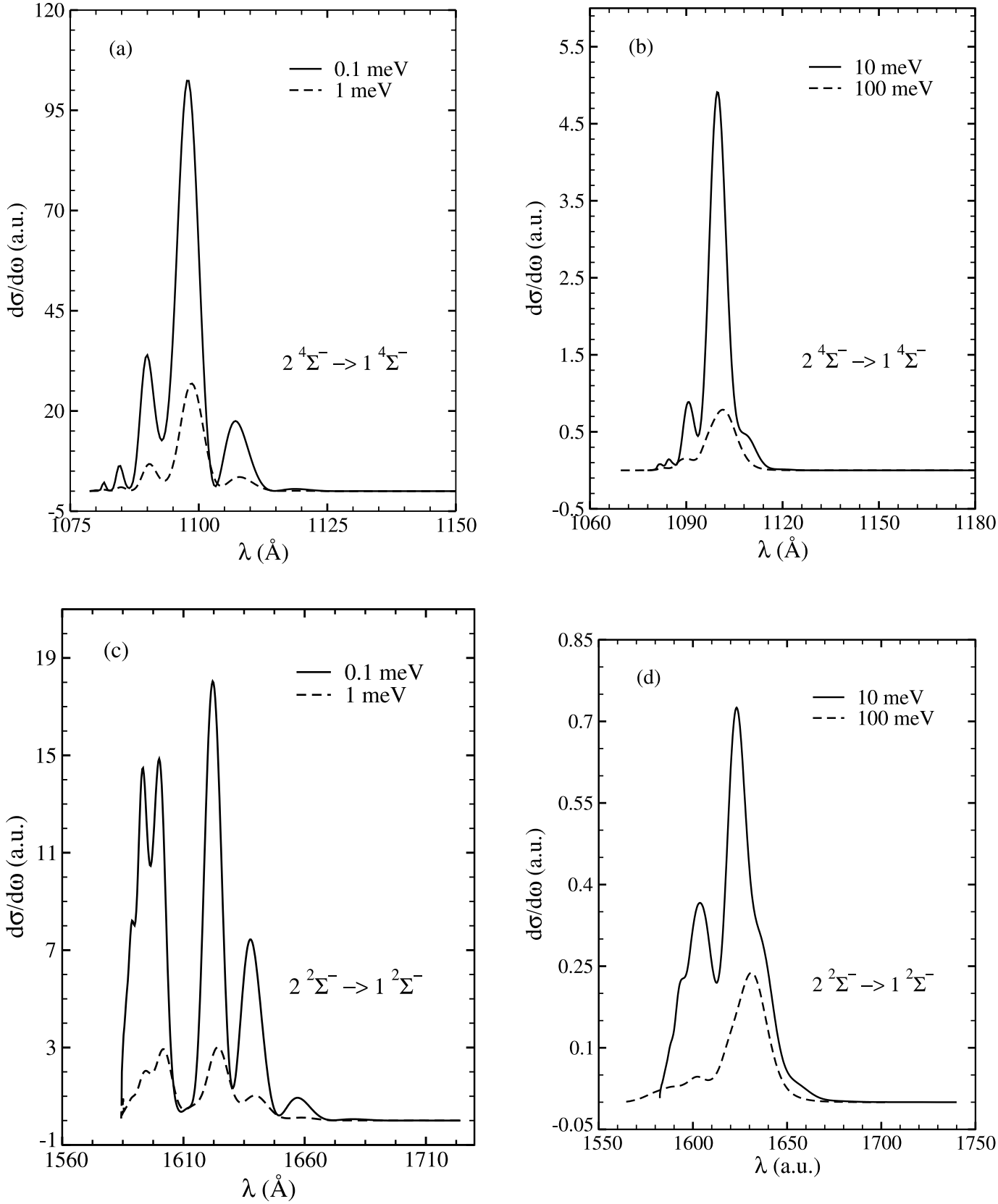

FIG. 6.—Total emission spectra for RCT in collisions of O(^3P) with He^+ at collision energies of 0.1, 1, 10, and 100 meV. (*a*, *b*) Transition $2\,^4\Sigma^- \rightarrow 1\,^4\Sigma^-$. (*c*, *d*) $2\,^2\Sigma^- \rightarrow 1\,^2\Sigma^-$.

the emitted photon (Zygelman et al. 1989). Therefore, an emission spectrum exhibits an oscillatory or resonance-like structure, as seen in Figure 6. We note that each partial wave for the transition $2\,^4\Sigma^- \rightarrow 1\,^4\Sigma^-$ has a structure similar to the total emission spectrum. The resonance-like structures are not related to quasi-bound states or orbiting in the exit channels, since the exit channels are nearly completely repulsive (see Table 2).

5. SUMMARY

Cross sections and rate coefficients have been presented for the radiative charge transfer process $O(^3P) + He^+ \rightarrow O^+(^4S^o, ^2P^o, ^2D^o) + He + \hbar\omega$. The calculations were performed with fully quantum mechanical, optical potential, and semiclassical methods. The cross sections were computed from 0.1 meV to $\sim$3 eV with the first two methods, but were extended to 10 keV with the semiclassical approach. Rate coefficients were obtained for temperatures between 10 and 10^6 K. The calculations demonstrate that direct charge transfer is negligible when compared to radiative decay for the temperature range considered. However, the rate coefficient for RCT is 6×10^{-15} cm^3 s^{-1} for temperatures relevant to the ejecta of Type II supernovae, 2 orders of magnitude too small to be an effective He^+ removal mechanism in unmixed regions. On the other hand, in chemically mixed ejecta models, in which the CO abundance is reduced, it may play a significant role in the chemistry. The total emission spectra for the two strongest transitions are also presented for several collision energies.

L. B. Z., P. C. S., and B. Z. acknowledge support from NASA grant NAG5-11453; R. J. B., H.-P. L., J. P. G., P. F., and Y. L. acknowledge financial support from the Deutsche Forschungsgemeinschaft grant Bu 450/7-3 and the Fonds der Chemischen Industrie; and M. K. acknowledges support from the Ministry of Education, Science, Sport, Culture, and Technology, Japan Society for Promotion of Science (JSPS) for the US-JP Collaborative Research Program, and Collaborative Research Grant by National Institute for Fusion Science.

APPENDIX

HÖNL-LONDON FACTORS

In this appendix, the expressions for the Hönl-London factors are obtained by deriving the expression for the radiative charge transfer cross section using the Fermi golden rule. In application of the Fermi golden rule, we must allow for the appropriate transformation between the molecular frame, in which the Born-Oppenheimer approximation is made, and the laboratory frame. Here we follow the procedure of Brown & Carrington (2003). Under such a transformation, the transition probability for radiative decay, integrated over all polarization directions, is written as

$$w_{ab} = \frac{4\omega^3}{3c^3} \sum_{pq} \left| \langle b | \mathcal{D}^1_{pq}(\Xi) \mathcal{M}^1_q | a \rangle \right|^2, \tag{A1}$$

where ω denotes the angular frequency of the emitted photon, c is the speed of light, $\mathcal{D}^{1*}_{pq}$ is the complex conjugate of the pq element of the first-rank rotation matrix tensor $\mathcal{D}^1$ with the Euler angles $\Xi = (\phi, \theta, \chi)$, $\mathcal{M}^1_q$ is the qth spherical component of the dipole operator, and $|a\rangle$ and $|b\rangle$ indicate the wave functions of the initial and final molecular states, respectively, defined by

$$|x\rangle = \psi^x_e(\boldsymbol{r}, R) \psi^x_{\rm rv}(R, \Xi) \tag{A2}$$

in the Born-Oppenheimer approximation (Brown & Carrington 2003) with $x = a, b$. In equation (A2), ψ^x_e is the electronic wave function of the molecular state, $\boldsymbol{r} = \{\boldsymbol{r}_1, \boldsymbol{r}_2, \boldsymbol{r}_3, \ldots\}$ are the coordinates of the molecular electrons, R is the internuclear distance, and $\psi^x_{\rm rv}$ is the rovibrational wave function of nuclear motion, written in the form

$$\psi^x_{\rm rv}(R, \Xi) = \frac{2\pi}{R} \sqrt{\frac{2\pi}{\mu k}} \sum_{JM} i^J e^{i\delta^x_J} f^x_J(k_x R) Y^*_{JM}(\theta_{k_x}, \phi_{k_x}) \mathfrak{D}^J_{M\Lambda}(\Xi), \tag{A3}$$

where δ^x_J denotes the phase shift corresponding to angular quantum number J, f^x_J is obtained from equation (9) with the asymptotic form given by equation (12), Y_{JM} is the spherical harmonic function, and $\mathfrak{D}^{J*}_{M,\Lambda}$ is the normalized rotational eigenfunction

$$\mathfrak{D}^J_{M,\Lambda}(\Xi)^* = \left[(2J+1)/8\pi^2\right]^{1/2} \mathcal{D}^J_{M,\Lambda}(\Xi)^*. \tag{A4}$$

Here the total angular momentum can be approximated by the rotational angular momentum. Except for the case of very low temperatures, this is a good approximation, as pointed out by Babb & Kirby (1998).

The cross section can be obtained by dividing equation (A1) by the flux density of the incident particles and integrating over the final states that conserve energy with the initial state,

$$\frac{d\sigma_{ab}}{d\omega} = \frac{4\omega^3}{3c^3} \int \frac{\mu}{(2\pi)^3 k_a} d\boldsymbol{k}_b \delta\left(\frac{k_b^2}{2\mu} - \frac{k_a^2}{2\mu} + \Delta E - \omega\right) \sum_{pq} \left| \langle b | \mathcal{D}^1_{pq}(\Xi) \mathcal{M}^1_q | a \rangle \right|^2, \tag{A5}$$

where $(2\pi)^{-3}$ is the density of the final states. Substituting equations (A2), (A3), and (A4) into equation (A5) leads to

$$\frac{d\sigma_{ab}}{d\omega} = \frac{8}{3}\left(\frac{\pi}{k_a}\right)^2 \frac{\omega^3}{c^3} \sum_{J,J'} \sum_{M,p} \mathfrak{M}_{J,J'}(k_a, k_b)(2J'+1) \left| \langle JM\Lambda | \mathcal{D}^k_{pq}(\Xi) | J'M'\Lambda' \rangle \right|^2, \tag{A6}$$

where $\mathfrak{D}^J_{M,\Lambda}(\Xi)$ is symbolized as $|JM\Lambda\rangle$, $\mathfrak{M}_{J,J'}$ is defined by equation (8) in which $D(R)$ is given by

$$D(R) = \int \psi^b_e(\boldsymbol{r}, R)^* \mathcal{M}^1_q \psi^a_e(\boldsymbol{r}, R) d\boldsymbol{r}, \tag{A7}$$

and $q = \Lambda - \Lambda'$ from the properties of 3-j symbols below. Adopting a useful relation for tensor operators (Brown & Carrington 2003),

$$\langle JM\Lambda | \mathcal{D}^k_{pq}(\Xi) | J'M'\Lambda' \rangle = (-1)^{M-\Lambda} [J, J']^{1/2} \begin{pmatrix} J & k & J' \\ -\Lambda & q & \Lambda' \end{pmatrix} \begin{pmatrix} J & k & J' \\ -M & p & M' \end{pmatrix}. \tag{A8}$$

Accordingly, the Hönl-London factors are determined by the equations below. For the $\Delta\Lambda = \Lambda - \Lambda' = 0$ case,

$$S^R_J(0) = \frac{(J'+1+\Lambda')(J'+1-\Lambda')}{J'+1}, \tag{A9}$$

$$S^Q_J(0) = \frac{(2J'+1)\Lambda'^2}{J'(J'+1)}, \tag{A10}$$

$$S^P_J(0) = \frac{(J'+\Lambda')(J'-\Lambda')}{J'}, \tag{A11}$$

for the $\Delta\Lambda = 1$ case,

$$S^R_J(1) = \frac{(J'+2+\Lambda')(J'+1+\Lambda')}{2(J'+1)}, \tag{A12}$$

$$S^Q_J(1) = \frac{(J'+1+\Lambda')(J'-\Lambda')(2J'+1)}{2J'(J'+1)}, \tag{A13}$$

$$S^P_J(1) = \frac{(J'-1-\Lambda')(J'-\Lambda')}{2J'}, \tag{A14}$$

and for the $\Delta\Lambda = -1$ case,

$$S^R_J(-1) = \frac{(J'+2-\Lambda')(J'+1-\Lambda')}{2(J'+1)}, \tag{A15}$$

$$S^Q_J(-1) = \frac{(J'+1-\Lambda')(J'+\Lambda')(2J'+1)}{2J'(J'+1)}, \tag{A16}$$

$$S^P_J(-1) = \frac{(J'-1+\Lambda')(J'+\Lambda')}{2J'}. \tag{A17}$$

In the above equations, R, Q, and P correspond to $\Delta J = J - J' = +1$, 0, and -1, respectively, and it should be emphasized that the expressions for the Hönl-London factors are the same as those given in Herzberg (1950), but differ by a factor of 1/2 in equations (A12)–(A17).

REFERENCES

Augustin, S. D., Miller, W. H., Pearson, P. K., & Schaefer, H. F. 1973, J. Chem. Phys., 58, 2845

Babb, J. F., & Kirby, K. P. 1998, in The Molecular Astrophysics of Stars and Galaxies, ed. T. W. Hartquist & D. A. Williams (Oxford: Clarendon), 11

Brown, J. M., & Carrington, A. 2003, Rotational Spectroscopy of Diatomic Molecules, (Cambridge: Cambridge Univ. Press)

Buenker, R. J. 1982, in Current Aspects of Quantum Chemistry 1981, ed. R. Carbo (Amsterdam: Elsevier), 17

Chambaud, G., Levy B., Launay, J. M., Millie, P., Roueff, E., & Tran Minh, F. 1980, J. Phys. B, 13, 4205

Cooper, D. L., & Wilson, S. 1981, Mol. Phys., 44, 161

Dalgarno, A., Du, M. L., & You, J. H. 1990, ApJ, 349, 675

Frenking, G., Koch, W., Cremer, D., Gauss, J., & Liebman, J. F. 1989, J. Phys. Chem., 93, 3397

Gearhart, R. A., Wheeler, J. C., & Swartz, D. A. 1999, ApJ, 510, 944

Gerardy, C. L., Fesen, R. A., Höflich, P., & Wheeler, J. C. 2000, AJ, 119, 2968

Gerardy, C. L., Fesen, R. A., Nomoto, K., Maeda, K., Höflich, P., & Wheeler, J. C. 2002, PASJ, 54, 905

Herzberg, G. 1950, Molecular Spectra and Molecular Structure, Vol. I: Spectra of Diatomic Molecules (2nd ed.; New York: Litton)

Kimura, M., Dalgarno, A., Chantranupong, L., Li, Y., Hirsch, G., & Buenker, R. J. 1993, ApJ, 417, 812

Kimura, M., Gu, J. P., Liebermann, H. P., Li, Y., Hirsch, G., Buenker, R. J., & Dalgarno, A. 1994, Phys. Rev. A, 50, 4854

Lepp, S., Dalgarno, A., & McCray, R. 1990, ApJ, 358, 262

Lin, S. L., & Bardsley, J. N. 1977, J. Chem. Phys., 66, 435

Liu, W., & Dalgarno, A. 1995, ApJ, 454, 472

Liu, W., Dalgarno, A., & Lepp, S. 1992, ApJ, 396, 679

Mott, N. F., & Massey, H. S. W. 1965, in The Theory of Atomic collisions (3rd ed.; Oxford: Oxford Univ. Press), 106

Oliva, E., Moorwood, A. F. M., & Danziger, I. J. 1987, Messenger, 50, 18
Pinto, P. A., & Woosley, S. E. 1988, Nature, 333, 534
Rank, D. M., Pinto, P. A., Woosley, S. E., Bregman, J. D., Witteborn, F. C., Axelrod, T. S., & Cohen, M. 1988, Nature, 331, 505
Simpson, R.W., Maclagan, R. G. A. R., & Harland, P. W. 1987, J. Chem. Phys., 87, 5419
Spyromilio, J., & Leibundgut, B. 1996, MNRAS, 283, L89
Spyromilio, J., Leibundgut, B., & Gilmozzi, R. 2001, A&A, 376, 188
Stancil, P. C., & Zygelman, B. 1996, ApJ, 472, 102
Viehland, L. A., & Mason, E. A. 1977, J. Chem. Phys., 66, 422
Viggiano, A. A., Morris, R. A., & Mason, E. A. 1993, J. Chem. Phys., 98, 6483
Zygelman, B., & Dalgarno, A. 1988, Phys. Rev. A, 38, 1877
Zygelman, B., Dalgarno, A., Kimura, M., & Lane, N. F. 1989, Phys. Rev. A, 40, 2340